Role of the mTOR-FOXO1 pathway in obesity-associated renal tubulointerstitial inflammation

HONG SUN[1], XINYU SHAO[1], JIAJIA HE[2], MICHAL GOLOS[3] and BIMIN SHI[1]

[1]Department of Endocrinology and Metabolism, The First Affiliated Hospital of Soochow University, Suzhou, Jiangsu 215006; [2]Department of Oncology, The Third Affiliated Hospital of Soochow University, The First People's Hospital of Changzhou, Changzhou, Jiangsu 213000, P.R. China; [3]Centre for Amyloidosis and Acute Phase Protein, Division of Medicine, University College London (UCL), London NW3 2PF, UK

Received August 5, 2018; Accepted November 13, 2018

DOI: 10.3892/mmr.2018.9727

Abstract. Since obesity is largely responsible for the growing incidence of renal tubulointerstitial inflammation, exploration into the mechanisms of obesity-associated tubulointerstitial inflammation is essential. Studies have demonstrated that mammalian target of rapamycin (mTOR) is a crucial molecule in the pathogenesis of renal inflammation, including regulating the expression of inflammatory factors. The purpose of the present study was to further elucidate the role of mTOR in obesity-associated tubulointerstitial inflammation. In the clinical study, obese and healthy subjects were recruited for physical examination, as well as the collection of blood and urine samples. Further study was performed on a high fat diet (HFD)-induced obese rat model and a cultured human renal tubular epithelial cell line (HK-2). The clinical study demonstrated that the participants with obesity had increased serum lipids, creatinine (Cr), urinary albumin to creatinine ratio (UACR) and urinary neutrophil gelatinase-associated lipocalin (u-NGAL). Moreover, the level of urinary monocyte chemoattractant protein-1 (u-MCP-1) was increased in the participants with obesity, and it was positively correlated with free fatty acid (FFA), UACR and u-NGAL. In the *in vivo* study, the results indicated that the levels of serum lipids, Cr and blood urea nitrogen (BUN), as well as 24 h urine protein and u-NGAL, were significantly increased in the HFD-fed obese rats. In addition, the infiltration of $CD68^+$ cells into the renal interstitial area and the release of interleukin-1β (IL-1β) was observed in the kidneys of obese rats. Meanwhile, the supernatant from HK-2 cells treated with palmitic acid stimulated THP-1 monocyte migration. The upregulation of MCP-1, phosphorylated forkhead boxO1 (p-FOXO1), and phosphorylated mTOR (p-mTOR) was observed *in vivo* and *in vitro*. However, inhibition of mTOR was able to alleviate the above effects. Overall, these results demonstrated that activated mTOR induced FOXO1 phosphorylation, which mediates renal MCP-1 release, causes tubulointerstitial inflammation and ultimately leads to pathological renal changes and dysfunction. However, inhibition of mTOR may play a renoprotective role during the progression of obesity-associated tubulointerstitial inflammation.

Correspondence to: Dr Hong Sun or Professor Bimin Shi, Department of Endocrinology and Metabolism, The First Affiliated Hospital of Soochow University, 188 Shizi Street, Suzhou, Jiangsu 215006, P.R. China
E-mail: sunhong@suda.edu.cn
E-mail: shibimin@163.com

Key words: obesity, renal tubulointerstitial inflammation, monocyte chemoattractant protein-1, forkhead boxO1, mammalian target of rapamycin

Introduction

Recent statistics from the Centers for Disease Control, the National Institutes of Health and the World Health Organization report that obesity has more than doubled since 1980, and almost two billion adults worldwide are overweight or obese (1). Obesity is a preventable disease; however, it is evident that current educational efforts have failed to counteract its upward trend. The growing epidemic of obesity in the world is a major factor in reducing life expectancy, and represents an economic burden and a serious health problem. It is largely responsible for the growing incidence and prevalence of diabetes, as well as cardiovascular and renal disease. Evidence indicates that obesity is a risk factor for the development of renal inflammation and dysfunction, that may progress towards chronic kidney disease (CKD) (2,3).

Considering that obesity is associated with a chronic low-grade inflammatory condition, and that studies have demonstrated that obesity-induced inflammation develops in the renal tubularinterstitium (4), exploring the mechanisms of the renal tubulointerstitial inflammatory response in obesity may be of particular importance. Multiple lines of evidence suggest that the direct action of monocyte chemoattractant protein-1 (MCP-1) is a powerful instigator of tubulointerstitial inflammation (5,6). Excessive MCP-1 in the renal interstitium may recruit macrophages and generate

inflammation, contributing to tubulointerstitial injury and the progression of CKD. Initially, circulatory MCP-1, produced and secreted by adipose tissue, had been the focus of attention as the root of tubulointerstitial inflammation. However, it has been reported that the concentrations of serum and urinary MCP-1 are not associated with each other in obesity, indicating a role for locally produced MCP-1 in the kidney (7). Therefore, research into the mechanisms of renal MCP-1 generation may be a useful step in understanding and developing novel treatments for human renal tubulointerstitial inflammation.

A previous study demonstrated that MCP-1 expression in the vascular smooth muscle cells of diabetic mice is negatively regulated by the transcription factor forkhead boxO1 (FOXO1) (8). Other reports have indicated that FOXO1 is able to regulate certain biological processes, including cell cycle arrest, DNA damage repair and oxidative stress inhibition (9-11). It has beneficial effects on renal injury by attenuating oxidative stress and inhibiting the activation of transforming growth factor beta-1 (TGF-β1) signaling in diabetic rats (12,13). However, whether FOXO1 is able to regulate MCP-1 production, thus mediating renal tubulointerstitial inflammation during obesity, is poorly understood. Furthermore, evidence shows that FOXO1 is a downstream target of mammalian target of rapamycin (mTOR) in human tracheal smooth muscle cells. When mTOR is activated by phosphorylation (p-mTOR), it stimulates FOXO1 phosphorylation (p-FOXO1) and translocation from the nucleus to the cytosol. In this case, FOXO1 is dissociated from the promoter of the target gene, enabling the gene to be expressed (14). Recent evidence demonstrates that mTOR serves a key role in the generation and development of renal inflammation, through functions such as NLRP3 inflammasome activation (15), and increasing autophagy in macrophages and renal cells (16), which mediates renal inflammatory cytokine release. Since mTOR is activated in obesity (17-19), the authors propose a possible scenario in which activated mTOR may enhance the phosphorylation of FOXO1, with p-FOXO1 subsequently dissociating from the MCP-1 promoter, followed by the increased expression of MCP-1, ultimately leading to a renal tubulointerstitial inflammatory response.

In the present study, renal function was initially evaluated in the participants with obesity, and the pathomorphology and associated mechanisms of tubulointerstitial inflammation were assessed in the high fat diet (HFD)-induced obese rat model and a cultured human renal tubular epithelial cell line (HK-2). The purpose of the current study was to provide insights into the onset of obesity-associated renal tubulointerstitial inflammation and to identify a potential novel approach to treating renal injury.

Materials and methods

Clinical study. A total of 35 subjects with obesity (19 males and 16 females) were recruited consecutively at the First Affiliated Hospital of Soochow University (Suzhou, China). The inclusion criteria were as follows: i) Obesity (BMI≥27 kg/m^2); and ii) Chinese adults (including mainland China, Taiwan, and individuals from Hong Kong living in Jiangsu) aged 18-65. The exclusion criteria were as follows: i) Diabetes mellitus; ii) currently taking drugs that might interfere with the study, such as statins, fibrates, steroids, antihypertensive or anti-diabetic agents; iii) interstitial pneumonia; iv) severe renal or liver disease; v) malignant tumors; and vi) a history of acute coronary syndrome, stroke or acute pancreatitis within 3 months prior to enrollment. In addition, 27 normal weight, healthy subjects (15 males and 12 females) with a BMI<24 kg/m^2 served as a control group. The Ethics Committee of the First Affiliated Hospital of Soochow University approved this study, and all subjects provided written informed consent. During the physical examination, body weight (BW), height and waist circumference (WC) were determined. Blood pressure (BP) was measured on the right arm using a standard mercury sphygmomanometer with the subject in a seated position after 10 min of rest. Venous blood samples were collected from overnight fasted subjects. Blood urea nitrogen (BUN), creatinine (Cr), total triglycerides (TG), total cholesterol (TC) and free fatty acid (FFA) were measured using a chemistry analyzer (Hitachi 7600; Hitachi, Ltd., Tokyo, Japan) at the central laboratory of the hospital. Urinary MCP-1 (u-MCP) and urinary neutrophil gelatinase-associated lipocalin (u-NGAL) concentrations were determined using ELISA kits (cat. no. ab179886, Abcam, Cambridge, UK; and cat. nos. SCB388Hu and SEB388Ra, Cusabio, Wuhan, China) according to the manufacturer's instructions. Urinary albumin was measured via the Coomassie brilliant blue method (cat. no. CO35-2; Nanjing Jiancheng Bioengineering Institute, Nanjing, China). The urinary albumin to creatinine ratio (UACR) was calculated from first voided spot samples using clean-catch techniques and sterile containers; ratios <30 mg/g creatinine were defined as normoalbuminuria, those between 30 and 300 mg/g creatinine as microalbuminuria, and those ≥300 mg/g creatinine as macroalbuminuria.

Animal model. Male Sprague-Dawley (SD) rats (5 weeks old; SIPPR-Bk Laboratory Animals Co., Ltd., Shanghai, China) weighing approximately 160 g were housed in polypropylene cages and maintained under controlled room temperature (22±2˚C) and humidity (60±5%) with a 12 h light/dark cycle. Housing and animal experiments were approved by the Committee for Animal Subjects at Soochow University according to institutional and national animal welfare guidelines. After one week of adaptation, rats were randomly assigned to receive a normal chow diet (NCD; D12102C; Research Diets, Inc., New Brunswick, NJ, USA) or a HFD (60% kcal in fat; D12492; Research Diets, Inc.) or HFD plus 1 mg/kg/day of specific mTOR inhibitor rapamycin (Rap; Sigma-Aldrich; Merck KGaA, Darmstadt, Germany) by intraperitoneal injection (HFD+Rap; n=5 rats per group) for 8 weeks (20,21). A 24 h urine sample was collected from the rats after 3 days of adaptation in individual metabolic cages to measure 24 h urine protein and u-NGAL levels. The rats were then weighed and sacrificed. Blood was collected to test Cr, BUN, TG, TC and FFA.

Renal histology. The kidneys were perfused with saline solution and then removed and weighed. Kidneys were fixed in 10% neutral formalin for 24 h at 4˚C and embedded in paraffin. Sequential paraffin-embedded tissue sections from

the renal cortex were cut. Cross-sections (3 μm) were placed on gelatin-coated slides and used for hematoxylin-eosin (HE) staining, periodic acid-silver methenamine (PASM) staining and immunohistochemical staining for CD68 (a macrophage marker). In each kidney, at least 20 non-overlapping cortical areas of tubulointerstitial section were analyzed. The remaining kidney tissue was snap-frozen in liquid nitrogen and stored at -80˚C for western blot analysis.

HE staining. The paraffin sections were stained using hematoxylin (cat. no. D006; Nanjing Jiancheng Bioengineering Institute) at room temperature for a total of 10 min, followed by washing under running water for 30-60 sec. The sections were then placed in eosin (cat. no. D006; Nanjing Jiancheng Bioengineering Institute) at room temperature for 1 min, followed by dehydration in a gradient of ethanol and clearing in xylene I and xylene II (cat. no. GD-RY1215-12; Shanghai Guduo Science and Technology Co., Ltd., Shanghai, China) twice for 1 min. Stained sections were observed and digital images were captured with a light microscope (magnification, x400; Zeiss GmbH, Jena, Germany).

PASM staining. Paraffin sections of each group were dewaxed in water, oxidized with a 0.5% periodic acid (cat. no. SBJ-0404; Nanjing SenBeiJia Biological Technology Co., Ltd, Nanjing, China) for 30 min, and washed under tap and distilled water. Following oxidization with 10% chromic acid (cat. no. 06; BaSiFu Co., Ltd, Nanjing, China) for 20 min, the sections were rinsed with distilled water, fixed in a 1% sodium sulfite solution (cat. no. SBJ-0628; Nanjing SenBeiJia Biological Technology Co., Ltd.) for 30 sec, washed with distilled water, and immersed under a hexamine-silver solution (cat. no. SBJ-0600; Nanjing SenBeiJia Biological Technology Co., Ltd.) for 30 min. The sections were left to stand at a temperature of 65˚C for a total of 4 min in a water bath, following which they were removed and washed with distilled water and measured under a microscope until the black precipitate appeared in the glomerular capillary basement membrane. Following the appearance of the black precipitate, the sections were colored using a 0.1% auric chloride solution (cat. no. G810493-5 g; Shanghai Chaoyan Biotechnology Co., Ltd., Shanghai, China) for 30 sec, washed under running water for 10 min, and stained with hematoxylin (cat. no. D006; Nanjing Jiancheng Bioengineering Institute) and 0.5% eosin for a total of 3 min. Upon completing a conventional dehydration cycle, the sections were cleared, sealed and observed, and digital images were captured with a light microscope (magnification, x400; Zeiss GmbH).

Immunohistochemical staining. Paraffin sections were routinely dewaxed into solution, blocked with 3% H_2O_2 methanol endogenous peroxidases (cat. no. AR1022; Wuhan Boster Biological Technology, Ltd., Wuhan, China), incubated with rabbit anti-rat CD68 monoclonal antibody (cat. no. ab125212; 1:50; Abcam) at 4˚C overnight, subsequently incubated with goat anti-rabbit secondary antibodies (cat. no. ab6721; 1:200; Abcam) at room temperature for 30 min, stained with DAB (cat. no. AR1022; Wuhan Boster Biological Technology, Ltd.), counterstained with hematoxylin (cat. no. D006; Nanjing Jiancheng Bioengineering Institute), and dried. Stained sections were observed and digital images were captured with a light microscope (magnification, x200; Zeiss GmbH).

Cell culture. HK-2 cells and a human monocyte cell line (THP-1) were obtained from the American Type Culture Collection (Manassas, VA, USA). HK-2 and THP-1 cells were cultured at 37˚C in RPMI 1640 medium (Lonza Group, Ltd., Basel, Switzerland) containing 10% fetal calf serum (HyClone; GE Healthcare Life Sciences, Logan, UT, USA), 2 mM L-glutamine solution, 100 U/ml penicillin and 100 μg/ml streptomycin (Sigma-Aldrich; Merck KGaA), in a cell culture incubator with 95% air and 5% CO_2 for 24 h. All experiments were performed in serum-free RPMI 1640 medium containing 0.2% bovine serum albumin (BSA; Sigma-Aldrich; Merck KGaA). Since palmitic acid (PA; Sigma-Aldrich; Merck KGaA) is a major constituent of FFA, it was used to treat the cells and simulate a high fat environment in the *in vitro* study (22,23).

Transwell filter migration assay and MCP-1 concentration detection. HK-2 cells were seeded in a 6-well plate at a density of $5x10^5$ cells/well and treated with the experimental medium in the absence or presence of 0.32 mM PA or 10 ng/ml Rap plus PA. After a 24-h incubation at 37˚C, culture supernatants were harvested via centrifugation at 1,000 x g at 37˚C for 10 min. Microporous membrane (pore size, 8 μm) Transwell inserts (Merck KGaA) were used for the chemotaxis assay. THP-1 cells ($5x10^4$) in 200 μl serum-free RPMI were added to the upper chamber, with 500 μl of the above culture supernatants in the lower chamber (HK-2 cells were treated with media containing 0.32 mM PA, 10 ng/ml Rap, or PA plus Rap; media without HK-2 cell treatment were used for a control experiment). THP-1 cells were allowed to migrate during a 2-h incubation at 37˚C with 5% CO_2, and then the inserts were fixed with methanol (cat. no. N168; Shanghai Chaoyan Biotechnology Co., Ltd.) for 20 min at room temperature and stained with 0.1% crystal violet for 10 min at room temperature (cat. no. C0775; Sigma-Aldrich; Merck KGaA). The non-migratory cells were removed prior to mounting of the membrane, and the number of migratory cells was observed under a light microscope (magnification, x200; Zeiss GmbH). MCP-1 in the supernatant was detected with an MCP-1 ELISA kit (cat. no. ab179886; Abcam), according to the manufacturer's protocol.

Small interfering (si)RNA transfection. HK-2 cells were cultured in six-well plates at a density of $5x10^5$ cells/well and transiently transfected with mTOR siRNA (sense, 5'-CCACCC GAAUUGGCAGAUUTT-3'; antisense, 5'-AAUCUGCCA AUUCGGGUGGTT-3'), FOXO1 siRNA (sense, 5'-GGAGGU AUGAGUCAGUAUATT-3'; antisense, 5'-UAUACUGACUCA UACCUCCTT-3') or empty vector siRNA (cat. nos. sc-35409 and sc-35382; Santa Cruz Biotechnology, Inc., Dallas, TX, USA) using Lipofectamine® 2000 (Invitrogen; Thermo Fisher Scientific, Inc., Waltham, MA, USA) following the manufacturer's protocol. Briefly, 1 μg siRNA was mixed with 6 μl Lipofectamine® 2000 and applied to the cells. The transfected cells were incubated at room temperature for 30 min and then seeded ($5x10^5$ cells) in a 6-well plate containing 900 μl

Table I. Baseline characteristics of obese and non-obese subjects.

Variables	Non-obese (n=27)	Obese (n=35)	P-value
Sex (male/female)	15/12	19/16	0.921
Age (years)	36±9	38±10	0.355
BMI (kg/m^2)	22.06±1.45	30.84±2.15[a]	<0.001
WC (cm)	77.33±6.76	117.80±5.03[a]	<0.001
SBP (mmHg)	110±4	123±15[a]	<0.001
DBP (mmHg)	72±7	82±9[a]	<0.001
TC (mmol/l)	3.37 (2.89, 4.02)	5.48 (3.25, 6.56)[a]	<0.001
TG (mmol/l)	1.51±0.47	3.29±1.47[a]	<0.001
FFA (mmol/l)	0.24±0.05	0.45±0.16[a]	<0.001
BUN (mmol/l)	4.13 (2.62, 5.43)	4.53 (2.56, 5.58)	0.452
Cr (μmol/l)	67.22±10.59	75.69±14.13[a]	0.012
UACR (mg/g)	4.67±2.35	45.88±37.15[a]	<0.001
u-NGAL (ng/ml)	6.65±2.25	22.18±15.14[a]	<0.001
u-MCP-1 (pg/ml)	196.23±61.54	293.02±100.19[a]	<0.001

The χ^2 test was applied to assess the distribution of sex between participants with obesity and the controls. TC and BUN data are expressed as the median and interquartile range, and statistical significance was determined by Kruskal-Wallis' test. All other data are expressed as the mean ± standard deviation; statistical significance was determined by Student's t-test. [a]P<0.05 vs. non-obese group. BMI, body mass index; WC, waist circumference; SBP, systolic blood pressure; DBP, diastolic blood pressure; TC, total cholesterol; TG, triglyceride; FFA, free fatty acid; BUN, blood urea nitrogen; Cr, creatinine; UACR, urinary albumin to creatinine ratio; u-MCP-1, urinary monocyte chemoattractant protein-1; u-NGAL, urinary neutrophil gelatinase-associated lipocalin.

Opti-MEM (Invitrogen; Thermo Fisher Scientific, Inc.). After a 24-h treatment with the experimental medium, the cells were harvested and examined by western blotting.

Protein extraction and western blot analysis. Cellular protein was extracted using a protein extraction kit (cat. no. W034; Nanjing SenBeiJia Biological Technology, Co., Ltd.) and total protein was quantified via a protein assay kit (bicinchoninic acid; cat. no. A045-4; Nanjing SenBeiJia Biological Technology Co., Ltd.). Total protein (30-80 μg) was subjected to electrophoresis on 6-15% SDS polyacrylamide gels. Proteins were transferred to polyvinylidene fluoride membranes, which were blocked for 1 h at room temperature with 5% BSA in Tris-buffered saline containing 0.05% Tween-20 (TBST). Subsequently, blots were washed and incubated overnight at 4˚C in TBST containing 5% bovine serum albumin with antibodies (1:1,000 dilution) against interleukin (IL)-1β (cat. no. ab9722; 1:1,000; Abcam), MCP-1 (cat. no. ab25124; 1:1,000; Abcam), p-FOXO1 (cat. no. ab131339; 1:1,000; Abcam), p-mTOR (cat. no. ab137133; 1:1,000; Abcam) and β-actin (cat. no. ab8227; 1:2,000; Abcam). Membranes were washed three times with TBST, incubated with a horseradish peroxidase-conjugated secondary antibody (cat. no. ab6721; 1:5,000; Abcam) for 1 h at room temperature and then washed three times again with TBST. Finally, detection procedures were performed using an enhanced chemiluminescence (ECL) Advance Western Blotting Detection kit and autoradiography was performed on Hyperfilm ECL (both GE Healthcare, Chicago, IL, USA). For quantitative analysis, bands were detected and evaluated by densitometry with LabWorks software 7.0 (UVP, LLC, Upland, CA, USA) and normalized to β-actin.

Statistical analysis. Statistical analyses were conducted using SPSS 18.0 (SPSS, Inc., Chicago, IL, USA). The χ^2 test was applied to assess the distribution of sex between participants with obesity and the controls. Normally distributed variables were analyzed with one-way analysis of variance (ANOVA) or Student's t-test. For variables with non-normal distribution, Kruskal-Wallis' test was used. Tukey's and Dunn's post hoc tests were used after the ANOVA and Kruskal-Wallis' test, respectively. Pearson's correlation analyses were used for continuous variables, and Spearman's correlation analyses were used for ranked variables. P<0.05 was considered to indicate a statistically significant difference.

Results

Baseline characteristics of obese and non-obese subjects. Table I presents the anthropometric and biochemical characteristics of the obese and non-obese subjects. Compared with non-obese controls, the participants with obesity had increased BMI, SBP and DBP, elevated TC, TG and FFA, as well as a larger WC. The Cr, UACR and u-NGAL were increased in the participants with obesity, while there was no significant difference in the BUN between the two groups (Table I). In addition, the participants with obesity had higher concentrations of u-MCP-1 (Table I), and the level of u-MCP-1 was positively correlated with FFA (r=0.507, P=0.002), UACR (r=0.550, P=0.001) and u-NGAL (r=0.448, P=0.007) in the participants with obesity (Fig. 1).

Biochemical characteristics of the rats. BW and the ratio of kidney weight (KW) to BW (KW/BW) was significantly increased in the HFD group, indicating that an obese rat model

Table II. Biochemical parameters of the NCD, HFD and HFD+Rap groups at the end of the intervention study (n=5).

				P-value	
Group	NCD	HFD	HFD+Rap	HFD vs. NCD	HFD+Rap vs. HFD
BW (g)	387.33±8.74	462.67±11.37[a]	459.67±4.51	0.001	0.693
KW/BW (%)	0.85±0.05	1.50±0.08[a]	1.22±0.10[b]	<0.001	0.016
TG (mmol/l)	0.35±0.05	1.81±0.03[a]	1.75±0.11	<0.001	0.405
TC (mmol/l)	1.60±0.10	10.97±0.75[a]	11.13±0.90	<0.001	0.818
FFA (mmol/l)	1.02±0.08	1.63±0.06[a]	1.63±0.08	<0.001	1.000
BUN (mmol/l)	5.23±0.35	10.33±0.61[a]	7.77±0.25[b]	<0.001	0.003
Cr (μmol/l)	34.67±1.53	68.33±1.53[a]	37.67±4.04[b]	<0.001	<0.001

Data are expressed as the mean ± standard deviation. Statistical significance was determined by one-way analysis of variance. [a]P<0.05 vs. NCD group; [b]P<0.05 vs. HFD group. BW, body weight; KW/BW, kidney weight/body weight; TG, triglyceride; TC, total cholesterol; FFA, free fatty acid; BUN, blood urea nitrogen; Cr, creatinine; NCD, normal chow diet; HFD, high fat diet; Rap, rapamycin.

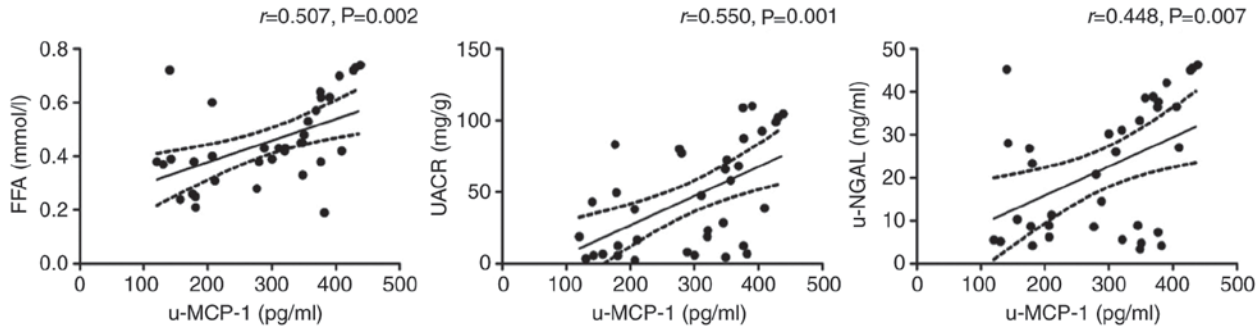

Figure 1. Pearson's correlation between u-MCP-1 levels and FFA, UACR and u-NGAL in patients with obesity. u-MCP-1, urinary monocyte chemoattractant protein-1; FFA, free fatty acid; UACR, urinary albumin to creatinine ratio; u-NGAL, urinary neutrophil gelatinase-associated lipocalin.

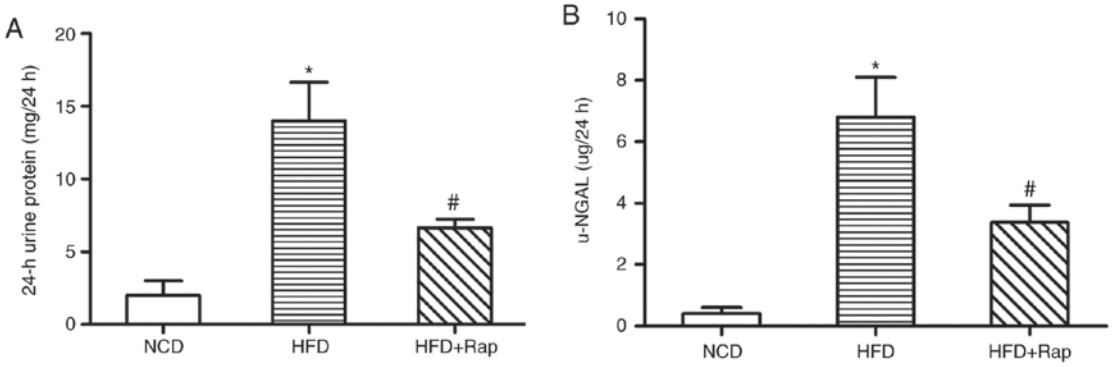

Figure 2. Levels of 24 h urine protein and u-NGAL levels. (A) Elevated 24 h urine protein and (B) u-NGAL levels in HFD-fed rats was alleviated by Rap treatment. Data are presented as the mean ± standard deviation of three individual experiments; statistical significance was determined by one-way analysis of variance. *P<0.05 vs. NCD group; #P<0.05 vs. HFD group. NCD, normal chow diet; HFD, high fat diet; Rap, rapamycin; u-NGAL, urinary neutrophil gelatinase-associated lipocalin.

was successfully established by HFD feeding. Moreover, the levels of serum TG, TC and FFA were markedly higher in HFD-fed rats compared with normal rats. Rap treatment reduced the KW/BW, although it did not notably affect the BW or serum lipids (Table II).

Renal function of the rats. The Cr, BUN, 24 h urine protein and u-NGAL in the HFD group was increased compared with the NCD group, indicating impaired renal function in these obese rats. By contrast, all the above effects were alleviated in the HFD+Rap group, suggesting that Rap improved the renal function of HFD-induced obese rats (Table II and Fig. 2).

Renal morphology and IL-1β expression in the rats. HE staining demonstrated vacuolar degeneration in the renal tubular epithelial cells of the HFD group, and PASM staining

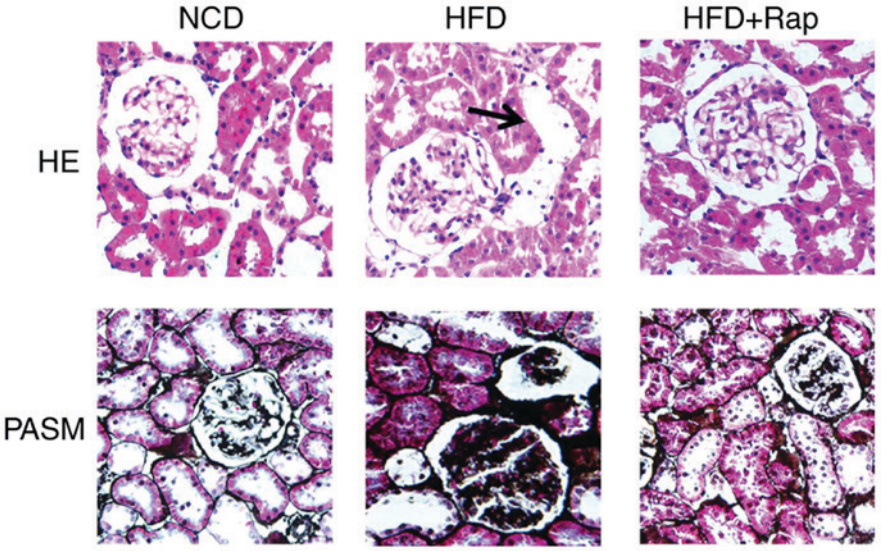

Figure 3. HE staining and PASM staining in rat kidney sections (magnification, x400). HE staining showed significant vacuolar degeneration in renal tubular epithelial cells of the HFD group (the black arrow), and PASM staining showed basement membrane thickening in the glomeruli and tubules of the HFD group. These pathological alterations were reduced by Rap treatment. HE, hematoxylin-eosin; PASM, periodic acid-silver methenamine; NCD, normal chow diet; HFD, high fat diet; Rap, rapamycin.

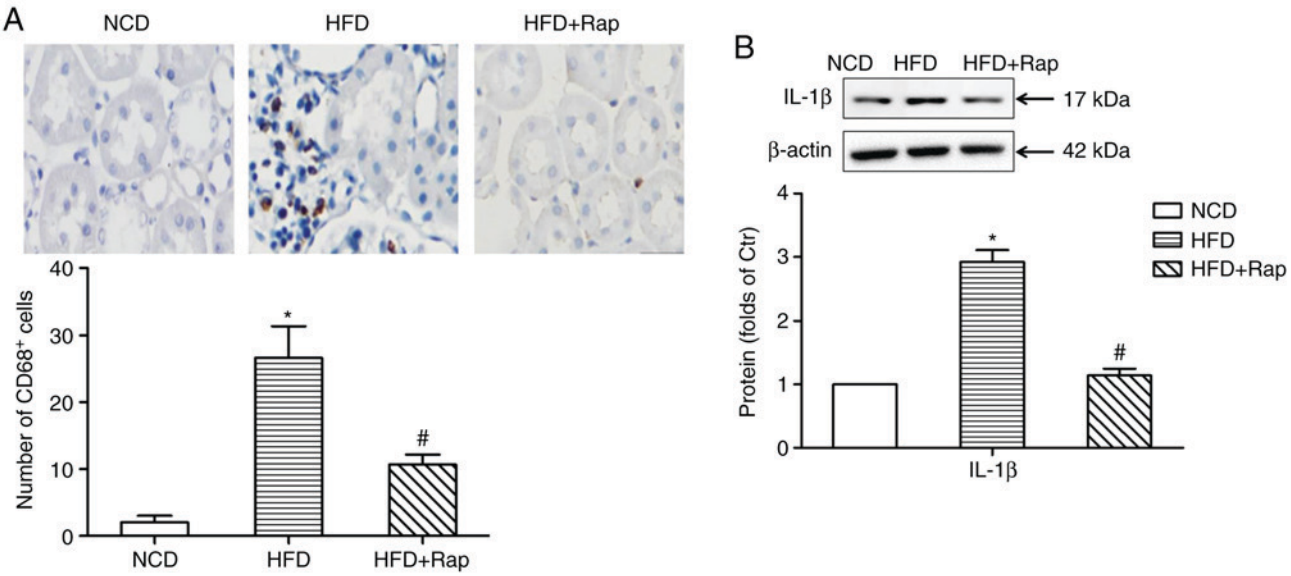

Figure 4. CD68 and IL-1β staining in rat renal sections. (A) Immunohistochemical staining for CD68 (magnification, x200). The HFD induced prominent infiltration of $CD68^+$ cells into the renal interstitial area, and Rap decreased the inflammatory cell infiltration. (B) The effects of Rap on the protein expression of IL-1β. Protein expression was examined by western blotting, normalized by comparison with β-actin and expressed as a percentage of control. Data are presented as the mean ± standard deviation of three individual experiments; statistical significance was determined by one-way analysis of variance. $^*P<0.05$ vs. NCD group; $^\#P<0.05$ vs. HFD group. NCD, normal chow diet; HFD, high fat diet; Rap, rapamycin; IL-1β, interleukin-1β.

highlighted basement membrane thickening in the glomeruli and tubules of HFD-fed rats, compared with the NCD group. These effects were alleviated by Rap treatment (Fig. 3). Immunohistochemical staining showed that there was prominent infiltration of $CD68^+$ cells (macrophages) into the renal interstitial area in the HFD group. The tubulointerstitial infiltration of inflammatory cells was significantly decreased by Rap treatment (Fig. 4A). Furthermore, the protein expression of IL-1β was increased in the kidneys of obese rats, compared with the NCD group, while Rap treatment inhibited the expression of IL-1β (Fig. 4B).

THP-1 monocyte migration. To assess whether PA and Rap were capable of affecting the migration of monocytes, supernatants from HK-2 cells treated with PA, PA plus Rap or Rap alone were tested for their ability to induce monocyte migration using a Transwell migration assay. The supernatants from HK-2 cells treated with PA stimulated THP-1 monocyte migration, and compared with PA, the PA+Rap group stimulated less monocyte migration (Fig. 5A). However, media containing PA, Rap or PA plus Rap that had not been exposed to HK-2 cells had no effect on THP-1 monocyte migration (Fig. 5B), suggesting that PA may mediate monocyte migration by

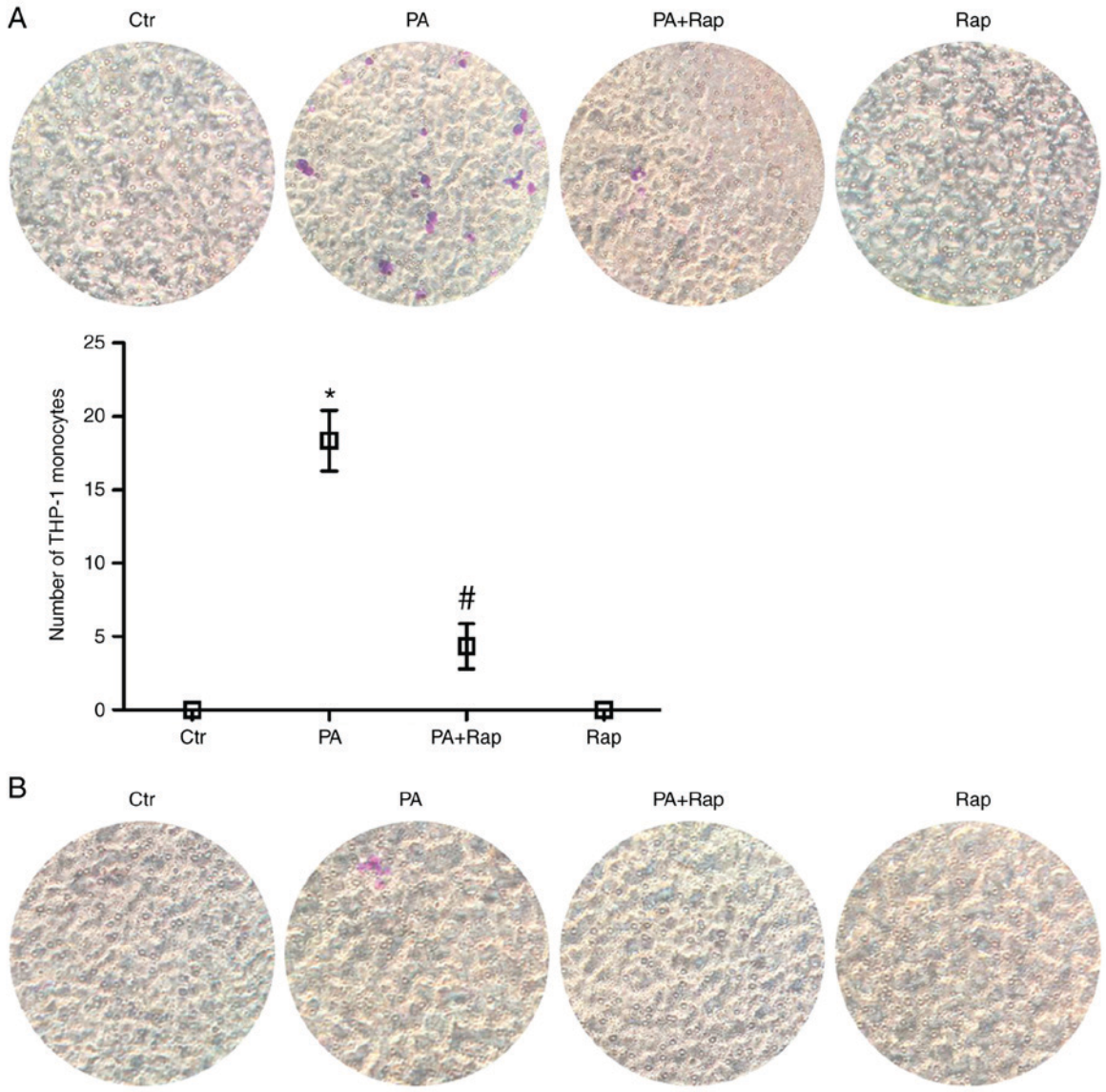

Figure 5. PA stimulates THP-1 monocyte migration. (A) HK-2 cells were treated with experimental medium (Ctr), and medium with 0.32 mM PA, 10 ng/ml Rap, or PA and 10 Rap. After a 24-h incubation, culture supernatants were harvested and used for the chemotaxis assay. The histogram represents the mean ± standard deviation of the THP-1 monocyte counts from three experiments, expressed as a percentage of the Ctr; statistical significance was determined by one-way analysis of variance. *P<0.05 vs. Ctr; #P<0.05 vs. PA. (B) The medium (Ctr) and media containing 0.32 mM PA, 10 ng/ml Rap or PA plus Rap without treating with HK-2 cells were used for a chemotaxis control assay. The media alone did not induce migration. Ctr, control; PA, palmitic acid; Rap, rapamycin.

stimulating the secretion of a certain type of chemokine from HK-2 cells, which is potentially inhibited by Rap.

Protein expression levels of MCP-1, p-FOXO1 and p-mTOR. To test the above hypothesis, the present study detected the expression of MCP-1 in the kidneys of HFD-induced obese rats and in HK-2 cells. The results demonstrated that the protein expression of MCP-1 was significantly increased in the kidneys of obese rats, while Rap treatment inhibited the expression of MCP-1 (Fig. 6A). In addition, PA induced the secretion of MCP-1 from the HK-2 cells, and this was inhibited by Rap, which was consistent with the induction of chemotaxis by the supernatants (Fig. 6B).

To investigate the potential mechanisms underlying this phenomenon, the protein expression of p-FOXO1 and p-mTOR was assessed *in vivo* and *in vitro*. It was found that p-FOXO1 and p-mTOR were upregulated at the protein level (Fig. 6A) in the kidneys of obese rats, while Rap treatment inhibited this change. The *in vitro* study showed that PA elevated the protein expression of p-FOXO1 and p-mTOR in HK-2 cells, which was inhibited by Rap. Compared with the control, Rap alone had no effect on the expression of these two molecules in HK-2 cells (Fig. 6C). mTOR siRNA or FOXO1 siRNA-transfected HK-2 cells were used to further confirm the above results. The data indicated that mTOR siRNA transfection downregulated the protein expression level of p-FOXO1 (Fig. 7A) and reduced the release of MCP-1 (Fig. 7B) in PA-treated HK-2 cells. Additionally, FOXO1 siRNA transfection increased the secretion of MCP-1 by the HK-2 cells, although not in the PA-treated HK-2 cells (Fig. 7B). Reduced protein expression of mTOR was also observed in the FOXO1 siRNA-transfected HK-2 cells with PA treatment (Fig. 7A).

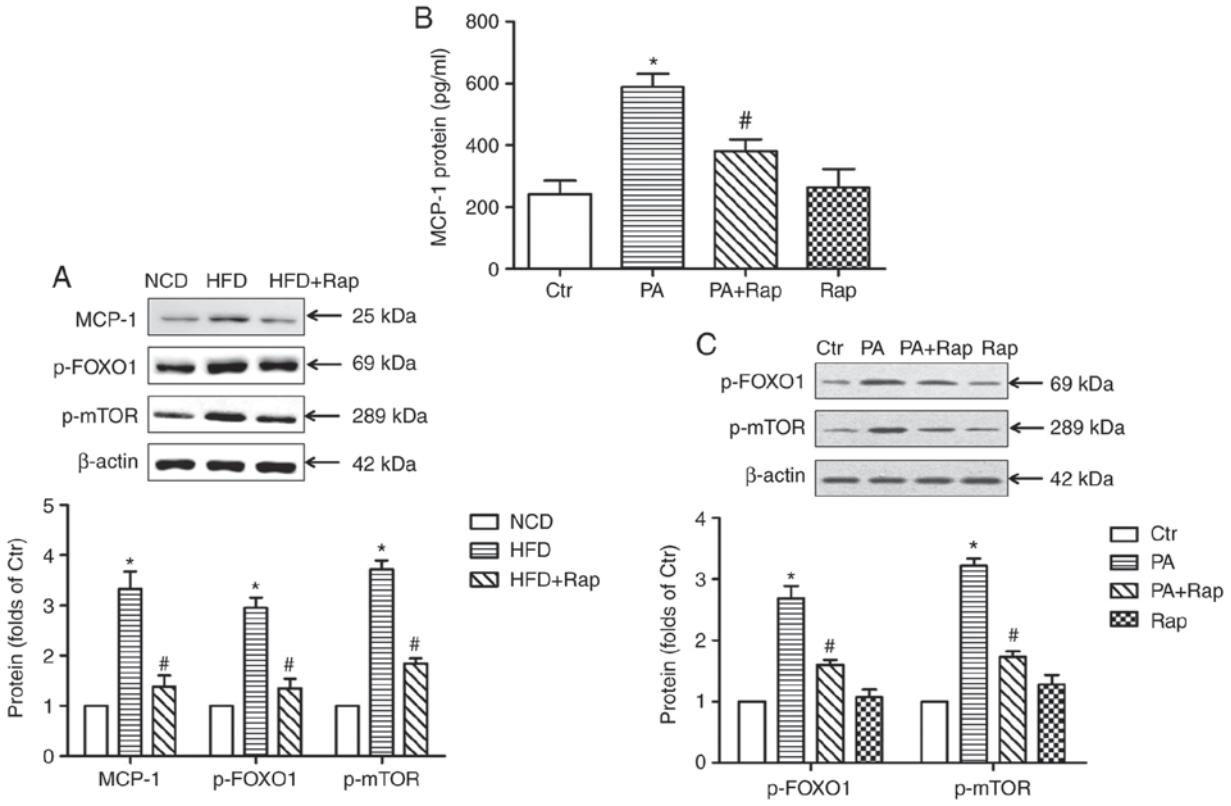

Figure 6. MCP-1, p-FOXO1 and p-mTOR expression in the kidneys of rats. (A) Protein expression was examined by western blotting, normalized by comparison with β-actin and expressed as a percentage of control. *P<0.05 vs. NCD group; #P<0.05 vs. HFD group. (B) The release of MCP-1 protein from HK-2 cells. MCP-1 protein content in the supernatant was detected with an ELISA kit. *P<0.05 vs. Ctr; #P<0.05 vs. PA. (C) The protein expression of p-FOXO1 and p-mTOR in HK-2 cells. Protein expression was examined by western blotting. *P<0.05 vs. Ctr; #P<0.05 vs. PA. Data are presented as the mean ± standard deviation of three individual experiments; statistical significance was determined by one-way analysis of variance. NCD, normal chow diet; HFD, high fat diet; Rap, rapamycin; MCP-1, monocyte chemoattractant protein-1; p-FOXO1, phosphorylated forkhead boxO1; p-mTOR, phosphorylated mammalian target of rapamycin; Ctr, control; PA, palmitic acid.

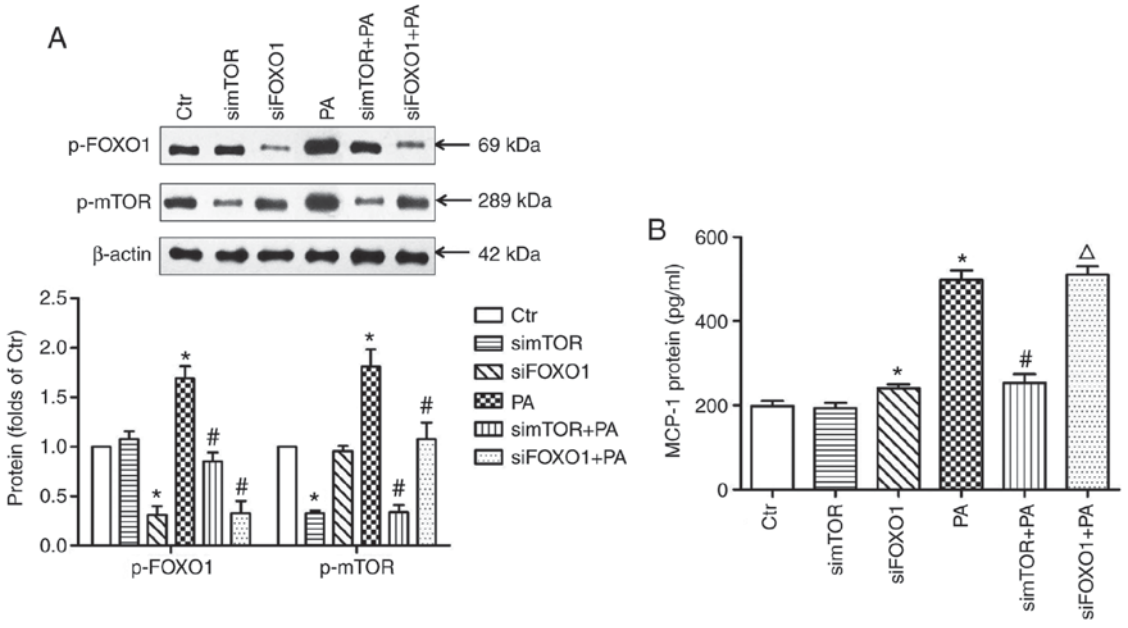

Figure 7. MCP-1, p-FOXO1 and p-mTOR expression in HK-2 cells transfected with mTOR siRNA or FOXO1 siRNA. (A) The protein expression of p-FOXO1 and p-mTOR in HK-2 cells transfected with mTOR siRNA or FOXO1 siRNA. Protein expression was examined by western blotting. *P<0.05 vs. Ctr; #P<0.05 vs. PA. (B) The release of MCP-1 from HK-2 cells transfected with mTOR siRNA or FOXO1 siRNA. MCP-1 protein content in the supernatant was detected with an ELISA kit. *P<0.05 vs. Ctr; #P<0.05 vs. PA; ΔP<0.05 vs. siFOXO1. Data are presented as the mean ± standard deviation of three individual experiments; statistical significance was determined by one-way analysis of variance. p-FOXO1, phosphorylated forkhead boxO1; p-mTOR, phosphorylated mammalian target of rapamycin; siRNA, small interfering RNA; Ctr, control; PA, palmitic acid; simTOR, siRNA targeting mammalian target of rapamycin; siFOXO1, siRNA targeting forkhead boxO1; HK-2, human renal tubular epithelial cell line; MCP-1, monocyte chemoattractant protein-1.

Discussion

Obesity, a chronic low-grade inflammatory condition, is associated with the development of numerous comorbidities, including renal disease. As more is understood about obesity, the perturbation of renal physiology in the context of obesity has become more apparent (24). In the present clinical study, dyslipidemia was observed in the participants with obesity, and these participants had higher Cr, UACR and u-NGAL, although not BUN, indicating that they had poorer renal function compared with those who were not obese, though not to a severe degree. In addition, the high level of u-MCP-1 was positively correlated with UACR and u-NGAL in the participants with obesity, suggesting that obesity-induced inflammatory responses may contribute to renal injury and dysfunction.

As it would be difficult to obtain kidney samples from the patients with simple obesity, an obese rat model was used to further investigate renal physiology and pathology. It was demonstrated that a HFD provoked overt obesity that was characterized by increased body weight, kidney weight gain and dyslipidemia. Early renal damage was also observed in the HFD-induced obese rats, as evidenced by elevated serum Cr and BUN levels, increased secretion of u-NGAL, proteinuria, vacuolar degeneration in the renal tubules, and glomerular and tubular basement membrane thickening. Additionally, infiltration of $CD68^+$ cells (macrophages) into the renal interstitial area and increased production of inflammatory factors (IL-1β) were found in the HFD-induced obese rats. Further *in vitro* study showed that supernatants from HK-2 cells treated with PA induced THP-1 monocyte migration. The above results indicated that the renal tubular cells may have been stimulated to release a particular type of chemokine. To explore this hypothesis, the expression of MCP-1 was assessed *in vivo* and *in vitro*, since MCP-1 serves an important role in renal inflammatory disease (25,26). The data illustrated that MCP-1 expression was significantly increased in the kidneys of HFD-induced obese rats and in the PA-treated HK-2 cells, which further confirmed the notable correlation between FFA and u-MCP-1 in the participants with obesity. Next, mTOR-FOXO1 signaling pathway protein expression was detected to gain an insight into the mechanism of MCP-1 secretion. The results demonstrated that the expression of p-FOXO1 was elevated in the kidneys of HFD-induced obese rats and in PA-treated HK-2 cells, suggesting that the increased p-FOXO1 had dissociated from the MCP-1 gene promoter and translocated from the nucleus to the cytosol, enabling MCP-1 to be expressed. In addition, the expression of p-mTOR was upregulated in the kidneys of HFD-induced obese rats and in PA-treated HK-2 cells. However, Rap inhibited the expression of MCP-1, p-FOXO1 and p-mTOR, and reduced the inflammatory cell infiltration and IL-1β release in the renal interstitium. Further data revealed that mTOR siRNA transfection downregulated the protein expression level of p-FOXO1 and reduced the release of MCP-1 from PA-treated HK-2 cells. These results suggested that the activated mTOR may have exerted adverse effects in obesity-associated renal tubulointerstitial inflammation. Furthermore, 8 weeks of Rap treatment lowered the Cr and BUN levels, reduced the secretion of urine protein and u-NGAL, improved vacuolar degeneration in the renal tubules and alleviated the glomerular and tubular basement membrane thickening in obese rats, suggesting that inhibition of mTOR may have exerted an anti-inflammatory effect to prevent obesity-associated renal tubulointerstitial inflammation. In the *in vitro* study, it was also identified that FOXO1 siRNA transfection increased MCP-1 release, indicating that FOXO1 silencing may have reduced MCP-1 promoter inhibition, and MCP-1 was consequently synthesized and secreted. Notably, FOXO1 siRNA transfection reduced the protein expression of p-mTOR in PA-treated HK-2 cells, which may explain the finding that no more MCP-1 was expressed in the PA+FOXO1 siRNA group compared with the PA group. Recently, certain reports have suggested a role for FOXO1 in renal protection (27,28). However, further investigation is required to explore whether FOXO1 is beneficial or detrimental in kidney diseases.

There are a number of limitations to the present study. First, the sample size of this hospital-based cross-sectional study was small, and larger samples are required in the future. Second, the obese animal model does not fully reflect the clinicopathological alterations in participants with obesity, and renal biopsy is necessary to investigate the pathological changes in the kidneys of patients with obesity. Third, other pro-inflammatory factors that have been associated with lower kidney function, such as TNF-α, were not evaluated in the present study (29).

In conclusion, the present findings provided novel evidence, to the best of our knowledge, that activated mTOR induced FOXO1 phosphorylation, which mediated renal MCP-1 release, caused tubulointerstitial inflammation and ultimately lead to renal pathological changes and dysfunction. The inhibition of mTOR may serve a renoprotective role during the progression of obesity-associated renal tubulointerstitial inflammation.

Acknowledgements

Not applicable.

Funding

This work was supported by the National Natural Science Youth Foundation of China (grant no. 81700632 to HS), the Natural Science Youth Foundation of Jiangsu Province (grant no. BK20170366 to HS), and the China Scholarship Council (CSC) (no. 201406090317).

Availability of data and materials

All data generated or analyzed during this study are included in this published article.

Authors' contributions

HS and BS designed the research; HS performed the research, analyzed the data and wrote the paper. XS, JH, MG and BS analyzed the data and revised the paper. All authors read and approved the final manuscript.

Ethics approval and consent to participate

The clinical study protocol was approved by the Institutional Review Board of The First Affiliated Hospital of Soochow

University and written informed consent was obtained from each subject. All human rights were observed in keeping with the Helsinki Declaration of 1975, as revised in 2008. The animal study was conducted in accordance with the ethical guidelines of the Declaration of Helsinki, the National Institutes of Health Guide for the Care and Use of Laboratory Animals and was approved by the Institutional Review Board of The First Affiliated Hospital of Soochow University.

Patient consent for publication

Not applicable.

Competing interests

The authors declare that they have no competing interests.

References

1. Chade AR and Hall JE: Role of the renal microcirculation in progression of chronic kidney injury in obesity. Am J Nephrol 44: 354-367, 2016.
2. Declèves AE and Sharma K: Obesity and kidney disease: Differential effects of obesity on adipose tissue and kidney inflammation and fibrosis. Curr Opin Nephrol Hypertens 24: 28-36, 2015.
3. Redon J and Lurbe E: The kidney in obesity. Curr Hypertens Rep 17: 555, 2015.
4. Li LC, Yang JL, Lee WC, Chen JB, Lee CT, Wang PW, Vaghese Z and Chen WY: Palmitate aggravates proteinuria-induced cell death and inflammation via CD36-inflammasome axis in the proximal tubular cells of obese mice. Am J Physiol Renal Physiol: Sep 19, 2018 (Epub ahead of print). doi: 10.1152/ajprenal.00536.2017.
5. Li A, Wang J, Zhu D, Zhang X, Pan R and Wang R: Arctigenin suppresses transforming growth factor-β1-induced expression of monocyte chemoattractant protein-1 and the subsequent epithelial-mesenchymal transition through reactive oxygen species-dependent ERK/NF-κB signaling pathway in renal tubular epithelial cells. Free radical research 49: 1095-1113, 2015.
6. Lv LL, Feng Y, Wen Y, Wu WJ, Ni HF, Li ZL, Zhou LT, Wang B, Zhang JD, Crowley SD and Liu BC: Exosomal CCL2 from tubular epithelial cells is critical for albumin-induced tubulointerstitial inflammation. J Am Soc Nephrol 29: 919-935, 2018.
7. Fu CP, Lee IT, Sheu WH, Lee WJ, Liang KW, Lee WL and Lin SY: The levels of circulating and urinary monocyte chemoattractant protein-1 are associated with chronic renal injury in obese men. Clin Chim Acta 413: 1647-1651, 2012.
8. Lu X, Yin D, Zhou B and Li T: miR-135a promotes inflammatory responses of vascular smooth muscle cells from db/db mice via downregulation of FOXO1. Int Heart J 59: 170-179, 2018.
9. Xing YQ, Li A, Yang Y, Li XX, Zhang LN and Guo HC: The regulation of FOXO1 and its role in disease progression. Life Sci 193: 124-131, 2018.
10. Puthanveetil P, Wan A and Rodrigues B: FoxO1 is crucial for sustaining cardiomyocyte metabolism and cell survival. Cardiovasc Res 97: 393-403, 2013.
11. Maiese K, Chong ZZ, Hou J and Shang YC: The 'O' class: Crafting clinical care with FoxO transcription factors. Adv Exp Med Biol 665: 242-260, 2009.
12. Qin G, Zhou Y, Guo F, Ren L, Wu L, Zhang Y, Ma X and Wang Q: Overexpression of the FoxO1 ameliorates mesangial cell dysfunction in male diabetic rats. Mol Endocrinol 29: 1080-1091, 2015.
13. Du M, Wang Q, Li W, Ma X, Wu L, Guo F, Zhao S, Huang F, Wang H and Qin G: Overexpression of FOXO1 ameliorates the podocyte epithelial-mesenchymal transition induced by high glucose in vitro and in vivo. Biochem Biophys Res Commun 471: 416-422, 2016.
14. Hsu CK, Lin CC, Hsiao LD and Yang CM: Mevastatin ameliorates sphingosine 1-phosphate-induced COX-2/PGE2-dependent cell migration via FoxO1 and CREB phosphorylation and translocation. Br J Pharmacol 172: 5360-5376, 2015.
15. Li X, Zhang X, Pan Y, Shi G, Ren J, Fan H, Dou H and Hou Y: mTOR regulates NLRP3 inflammasome activation via reactive oxygen species in murine lupus. Acta Biochim Biophys Sin (Shanghai) 50: 888-896, 2018.
16. Zhang X, Howell GM, Guo L, Collage RD, Loughran PA, Zuckerbraun BS and Rosengart MR: CaMKIV-dependent preservation of mTOR expression is required for autophagy during lipopolysaccharide-induced inflammation and acute kidney injury. J Immunol 193: 2405-2415, 2014.
17. Jiang H, Westerterp M, Wang C, Zhu Y and Ai D: Macrophage mTORC1 disruption reduces inflammation and insulin resistance in obese mice. Diabetologia 57: 2393-2404, 2014.
18. Paschoal VA, Amano MT, Belchior T, Magdalon J, Chimin P, Andrade ML, Ortiz-Silva M, Castro É, Yamashita AS, Rosa Neto JC, *et al*: mTORC1 inhibition with rapamycin exacerbates adipose tissue inflammation in obese mice and dissociates macrophage phenotype from function. Immunobiology 222: 261-271, 2017.
19. Perl A: mTOR activation is a biomarker and a central pathway to autoimmune disorders, cancer, obesity, and aging. Ann N Y Acad Sci 1346: 33-44, 2015.
20. Yang P, Xiao Y, Luo X, Zhao Y, Zhao L, Wang Y, Wu T, Wei L and Chen Y: Inflammatory stress promotes the development of obesity-related chronic kidney disease via CD36 in mice. J Lipid Res 58: 1417-1427, 2017.
21. Wang B, Ding W, Zhang M, Li H and Gu Y: Rapamycin attenuates aldosterone-induced tubulointerstitial inflammation and fibrosis. Cell Physiol Biochem 35: 116-125, 2015.
22. Lu Y, Cheng J, Chen L, Li C, Chen G, Gui L, Shen B and Zhang Q: Endoplasmic reticulum stress involved in high-fat diet and palmitic acid-induced vascular damages and fenofibrate intervention. Biochem Biophys Res Commun 458: 1-7, 2015.
23. Mu Y, Yin TL, Yin L, Hu X and Yang J: CTRP3 attenuates high-fat diet-induced male reproductive dysfunction in mice. Clin Sci (Lond) 132: 883-899, 2018.
24. Ting SM, Nair H, Ching I, Taheri S and Dasgupta I: Overweight, obesity and chronic kidney disease. Nephron Clin Pract 112: C121-C127, 2009.
25. Haller H, Bertram A, Nadrowitz F and Menne J: Monocyte chemoattractant protein-1 and the kidney. Curr Opin Nephrol Hypertens 25: 42-49, 2016.
26. Lv W, Booz GW, Wang Y, Fan F and Roman RJ: Inflammation and renal fibrosis: Recent developments on key signaling molecules as potential therapeutic targets. Eur J Pharmacol 820: 65-76, 2018.
27. Chen P, Shi X, Xu X, Lin Y, Shao Z, Wu R and Huang L: Liraglutide ameliorates early renal injury by the activation of renal FoxO1 in a type 2 diabetic kidney disease rat model. Diabetes Res Clin Pract 137: 173-182, 2018.
28. Hong YA, Bae SY, Ahn SY, Kim J, Kwon YJ, Jung WY and Ko GJ: Resveratrol ameliorates contrast induced nephropathy through the activation of SIRT1-PGC-1α-Foxo1 signaling in mice. Kidney Blood Press Res 42: 641-653, 2017.
29. Mehaffey E and Majid DSA: Tumor necrosis factor-α, kidney function, and hypertension. Am J Physiol Renal Physiol 313: F1005-F1008, 2017.